PARAMETRIZATION OF CROSS SECTIONS FOR NEUTRON INTERACTION WITH ^{1}H, ^{2}H and ^{12}C NUCLEI AT ENERGIES BETWEEN 20 AND 90 MeV*

J. BALEWSKI, K. BODEK, L. JARCZYK, B. KAMYS

AND

A. STRZAŁKOWSKI

Institute of Physics, Jagellonian University
Reymonta 4, 30-059 Kraków, Poland

(Received November 15, 1990)

The experimental data for neutron interaction with ^{1}H, ^{2}H and ^{12}C nuclei are parametrized in energy range 20 to 90 MeV. The energy dependence of the total and reaction cross section is represented in the form of a series of orthogonal polynomials. The logarithm of differential cross section for the angular distribution is expressed as a linear combination of Legendre polynomials with the energy dependence of their coefficients described by a series of orthogonal polynomials.

PACS numbers: 25.40.Dn, 25.40.Fq

1. Introduction

Recently, experiments concerning neutron elastic scattering and neutron induced breakup of deuteron have been extended to energies up to 100 MeV [1]. For reliable analysis of such experiments the efficiency of neutron detectors with scintillators containing ^{1}H, ^{2}H and ^{12}C nuclei has to be determined and the effects of neutron multiple scattering in the experimental equipment have to be known. The knowledge of total and differential cross sections for processes in n+^{1}H, n+^{2}H and n+^{12}C systems in the broad neutron energy range is necessary for such calculations in the framework of the Monte Carlo simulation method.

* This work has been supported by Polish Ministry of National Education under contract CPBR RRI.14 and CPBP 01.09.

The existing experimental data at neutron energies higher than 20 MeV are scarce and scattered in various journals. They are usually published in the form of diagrams or numerical tables. The practical use of such information is not straightforward, especially when some interpolation or extrapolation is necessary. Therefore, a parametrization of the available experimental cross sections is very desirable.

In the present work the parametrization of total and differential cross sections for the processes induced by neutrons on ^{1}H and ^{12}C nuclei has been performed in 20–90 MeV neutron energy range. For ^{2}H target nuclei the elastic scattering angular distribution was parametrized in energy range from 2–90 MeV. Total and total reaction cross sections have been considered as a function of energy for all these systems. Energy and angle dependence of differential cross sections for elastic scattering have been also parametrized.

Some attempts of a similar parametrization have been performed recently [2], [3] with the aim to use it in the Monte Carlo calculations of neutron detector efficiency. Del Guerra published the compilation [2] of the total and reaction cross sections for n+^{1}H and n+^{12}C systems at neutron energies up to 300 MeV. This complication has concerned only the total (*i.e.* angle integrated) cross sections; the angular distributions have been not considered. Another compilation, published by Uwamino *et al.* [3], concerns again total and reaction cross sections for n+^{1}H and n+^{12}C systems as a function of neutron energy in the range of 1–100 MeV. Angular distributions for elastically scattered neutrons on ^{12}C have been represented by the expansion in the series of Legendre polynomials (with the highest polynomial order up to nine). This expansion was inadequate to represent properly the experimental angular distributions at higher energies.

These two [2], [3] compilations do not include interaction of neutrons with deuterons and neglect the angular dependence of the differential cross sections for reactions on ^{1}H and on ^{12}C targets [2] or treat it only approximately [3]. Thus, they are not sufficient for the purpose of the Monte Carlo simulation for effects of multiple scattering of high energy neutrons. Moreover, they cannot be used for a simulation of the neutron interaction with the targets and detectors containing deuterons.

The parametrization proposed in the present paper removes these deficiencies. Experimental data published in the literature (see Tables I, II and III) are used as the input data. The energy dependence of the total or reaction cross sections was parametrized in the form of a series of orthogonal polynomials. The logarithm of the differential cross section for experimental angular distributions is represented as a linear combination of the Legendre polynomials, with the energy dependence of the expansion coefficients described by a series of orthogonal polynomials.

TABLE I

Experimental data for n + ^{1}H scattering analyzed in the present work

E_{lab} [MeV]	Measured quantity	Number of data points	Ref.
20.	TOT	1	[4]
19. ÷ 96.	TOT	50	[31]
20.	DIF 0 ÷ 180°	–	[4]
25.8	DIF 20 ÷ 178°	16	[32]
27.5	DIF 7 ÷ 173°	11	[7]
32.5	DIF 7 ÷ 173°	15	[7]
37.5	DIF 7 ÷ 173°	17	[7]
39.4	DIF 6 ÷ 173°	17	[8]
40.	DIF 62 ÷ 170°	12	[9]
42.5	DIF 7 ÷ 173°	22	[7]
47.5	DIF 7 ÷ 173°	22	[7]
50.	DIF 20 ÷ 173°	20	[32]
52.5	DIF 7 ÷ 173°	23	[7]
57.5	DIF 7 ÷ 173°	23	[7]
60.9	DIF 0 ÷ 170°	14	[10]
62.5	DIF 7 ÷ 173°	23	[7]
63.1	DIF 39 ÷ 160°	19	[11]
70.	DIF 6 ÷ 173°	22	[8]
70.	DIF 7 ÷ 173°	24	[7]
80.	DIF 7 ÷ 173°	24	[7]
89.5	DIF 7 ÷ 173°	24	[7]
95.0	DIF 7 ÷ 173°	19	[8]

TOT — total integrated cross section
DIF — differential cross section for elastic scattering
$\vartheta_1 \div \vartheta_2$ — CM angular range of experimental data

TABLE II

Experimental data for n + ^{2}H scattering analyzed in the present work

E_{lab} [MeV]	Measured quantity	Number of data points	Ref.
22. ÷ 98.	TOT	24	[12]
24. ÷ 60.	TOT	8	[13]
18. ÷ 46.	TOT	5	[14]
18. ÷ 40.	TOT	8	[15]
20.	TOT	1	[16]

TABLE II continued

E_{lab} [MeV]	Measured quantity	Number of data points	Ref.
3.4	REACT	1	THRESHOLD
3.5 ÷ 30.	REACT	18	[15]
14. ÷ 46.	REACT	5	[14]
6. ÷ 14.	REACT	6	[17]
77., 95.	REACT	2	[17]*
2.	DIF 69 ÷ 139°	14	[16]
2.22	DIF 60 ÷ 180°	13	[18]
2.45	DIF 24 ÷ 164°	9	[16]
2.5	DIF 69 ÷ 138°	13	[16]
2.5	DIF 66 ÷ 142°	7	[15]
3.	DIF 66 ÷ 179°	9	[15]
3.22	DIF 49 ÷ 164°	11	[16]
3.27	DIF 31 ÷ 164°	8	[16]
3.5	DIF 66 ÷ 179°	9	[15]
4.	DIF 66 ÷ 179°	10	[15]
4.5	DIF 66 ÷ 179°	11	[15]
4.95	DIF 53 ÷ 180°	26	[18]
5.	DIF 66 ÷ 179°	12	[15]
5.5	DIF 70 ÷ 172°	7	[16]
5.55	DIF 46 ÷ 146°	10	[14]
5.64	DIF 49 ÷ 146°	21	[18]
6.	DIF 66 ÷ 179°	12	[15]
7.	DIF 45 ÷ 179°	13	[15]
7.	DIF 46 ÷ 156°	10	[14]
7.01	DIF 52 ÷ 149°	19	[18]
8.	DIF 45 ÷ 179°	13	[15]
8.	DIF 46 ÷ 151°	11	[14]
9.	DIF 46 ÷ 179°	13	[15]
9.	DIF 46 ÷ 156°	9	[14]
10.25	DIF 46 ÷ 179°	14	[15]
12.	DIF 46 ÷ 179°	14	[15]
14.	DIF 46 ÷ 179°	13	[15]
14.1	DIF 46 ÷ 177°	25	[16]
14.2	DIF 23 ÷ 180°	15	[18]
14.3	DIF 14 ÷ 152°	19	[18]
16.	DIF 46 ÷ 179°	13	[15]
18.	DIF 44 ÷ 179°	13	[15]
18.55	DIF 42 ÷ 156°	23	[14]
20.	DIF 44 ÷ 179°	13	[15]
20.5	DIF 45 ÷ 154°	22	[14]

TABLE II continued

E_{lab} [MeV]	Measured quantity	Number of data points	Ref.
22.5	DIF $44 \div 179°$	13	[15]
23.	DIF $45 \div 155°$	17	[14]
25.	DIF $44 \div 179°$	12	[15]
27.5	DIF $44 \div 179°$	12	[15]
30.	DIF $44 \div 179°$	11	[15]
36.	DIF $19 \div 180°$	18	[14]
46.3	DIF $25 \div 180°$	17	[14]
49.4	DIF $30 \div 170°$	17	[14]*
64.8	DIF $30 \div 169°$	46	[19]*
77.	DIF $30 \div 160°$	17	[20]*
95.	DIF $30 \div 160°$	14	[21]*

REACT — reaction integrated cross section
* — proton induced reaction
TOT, DIF, $\vartheta_1 \div \vartheta_2$ — as in Table I

TABLE III

Experimental data for n + ^{12}C scattering analyzed in the present work

E_{lab} [MeV]	Measured quantity	Number of data points	Ref.
20.	TOT	1	[4]
19. ÷ 96.	TOT	51	[31]
25. ÷ 59.	TOT	8	[22]
95.	TOT	1	[27]
20.	REACT	1	[4]
19. ÷ 96.	REACT	26	[23]
21. ÷ 29.	REACT	3	[24]
40., 50.	REACT	2	[25]
55., 81.	REACT	2	[26]
95.	REACT	1	[27]
21. ÷ 84.	DIF $15 \div 85°$	*	[5]

* — 19 angular distributions [5] have been used to determine parameters of the p + ^{12}C optical model potential. The potential has been applied (with the switched off Coulomb part) for generation of n+ ^{12}C angular distribution as described in text,
REACT — as in Table II,
TOT, DIF, $\vartheta_1 \div \vartheta_2$ — as in Table I

The proposed parametrization of the cross sections valid for energies 20–90 MeV was matched to the parametrization given by Dietze and Klein [4] for ^{1}H and ^{12}C target nuclei in the neutron energy range: 0.1÷20 MeV. Our parametrization for the n+^{2}H total cross section was matched to the Horsley parametrization [16] based on a large body of experimental data obtained for neutron energies in 0.1÷20 MeV range.

Proposed parametrization enables us to perform the Monte Carlo simulation of neutron interaction with ^{1}H, ^{2}H and ^{12}C nuclei at high neutron energies.

The next paragraphs contain description of the input data and applied procedure. The results of the parametrization are presented in the graphical form. The numerical values of the coefficients are available on demand.

2. Input experimental data

The information on experimental data used as the input for the cross section parametrization is gathered in Tables I, II and III for the nuclei ^{1}H, ^{2}H and ^{12}C, respectively. The energy of neutron is listed in the first column, symbol of measured quantity in the second, number of experimental data in the third and reference number to the literature in the fourth column.

The experimental errors reported in the literature were taken to determine the weights of data used for parametrization, and in case when data had to be read out from the published curves, the errors were assumed to be 10%.

For n+^{1}H system the data contain only the cross sections for elastic scattering. The probability of other processes, as *e.g.* radiative capture, has been neglected, thus the total cross section was assumed to be equal to the total elastic cross section.

The data for n+^{1}H system at 20 MeV were taken from [4] in order to match our parametrization with that of this reference. The error of this data was assumed to be 2%. Data from Refs [8] and [9] were read out from figures.

In the case of n+^{2}H system the total cross section can be decomposed into two leading parts: those for elastic and break up reactions. The other processes are negligible for neutron energy below 90 MeV. The total cross section at 20 MeV was taken from Ref. [16], to match our parametrization with that of this reference. The error of it was assumed to be 0.2%.

In order to force the parametrization to follow the cross section near reaction threshold (3.34 MeV), an additional point of reaction cross section at energy 3.4 MeV with value 1.0±0.1 mb was included in fitting procedure. At energies 77 and 95 MeV, where n+^{2}H data were not available, the reaction cross sections for p+^{2}H system from Ref. [17] were taken instead. Data from Refs [14,16,18–21] and [27] were read out from figures.

The n+^{2}H elastic scattering differential cross sections were replaced by those for p+^{2}H system above $\vartheta_{cm} = 30°$ from Refs [19,20] and [21], to compensate the lack of appropriate experimental n+^{2}H data. It has been shown in Ref. [14] that differences between elastic angular distribution for n+^{2}H and p+^{2}H for ϑ_{cm} greater than 30° are small for energy greater than 46 MeV.

For the n+^{12}C system only the elastic scattering data and total reaction cross section were parametrized as a function of energy; no attempt was made to decompose the last one into cross sections for different reaction channels. The data at 20 MeV were taken from Ref. [4], to match our parametrizations with that of this reference. The error for this point was assumed to be 0.7%. We used 61 data points for total cross section parametrization from Refs [4,22,27] and [31]. The data from Ref. [22] (8 points) had very small errors in comparison to other data. We increased errors of these points 10 times to make their weights comparable with others during fitting procedure.

Because of insufficient experimental data on angular distributions for elastic scattering in n+^{12}C system above 40 MeV, the n+^{12}C data were replaced by those for p+^{12}C [5] measured between 21.1 MeV and 83.4 MeV.

3. Parametrization of the total cross section

The energy dependence of the total cross section has been represented by the expression:

$$\sigma(E) = \frac{1}{\sqrt{E}} \left(\sum_{k=0}^{K_{max}} A_k Q_k(\tilde{E}) \right) , \tag{1}$$

where $\tilde{E} \equiv E/50 - 1$ is the "reduced energy" introduced to transform the argument value of orthogonal polynomials to the interval $(-1, 1)$ (this is useful for numerical purposes), and $Q_k(\tilde{E})$ are orthogonal polynomials defined by the following formula:

$$\sum_{i=1}^{N_{data}} W_i Q_j(\tilde{E}_i) Q_k(\tilde{E}_i) = 0 \qquad (j \neq k) ,$$

$$Q_0(\tilde{E}) = 1 . \tag{2}$$

$(E_i, \quad i = 1, N_{data})$ is a set of energy values at which the experimental data have been measured, $(W_i, \quad i = 1, N_{data})$ are weights of individual data points defined by the experimental errors of cross sections:

$$W_i = (\Delta\sigma_i)^{-2} . \tag{3}$$

The polynomials Q_j satisfy the recursive relation:

$$Q_j(\tilde{E}) = (\tilde{E} - R_j)Q_{j-1}(\tilde{E}) + S_jQ_{j-2}(\tilde{E}) \qquad (j = 1,\ 2, \ldots),$$

$$Q_0(\tilde{E}) \equiv 1, \qquad Q_{-1}(\tilde{E}) \equiv 0. \qquad (4)$$

Coefficients R_j and S_j have been evaluated according to formulae given in Ref. [6].

The quality of the obtained fits is illustrated by Fig. 1. The experimental total cross sections are shown as points while the fitted interpolating curve is presented by solid line. The dashed lines show the range of three standard deviations of the fitted curve. These deviations have been calculated using the theorem of error propagation when the best fit value of the

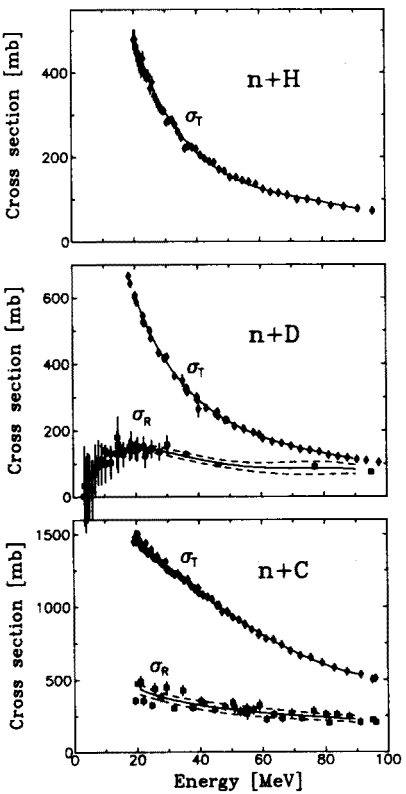

Fig. 1. Parametrization of energy dependence of total σ_T and reaction cross section σ_R for n+^{1}H, n+^{2}H and n+^{12}C systems. The experimental data (points) were fitted by means of formula (1), (solid line). Dashed lines show the range of 3 standard deviations of the fitted lines.

minimized χ^2-function,

$$\chi^2 = \frac{1}{N_{\text{data}} - K_{\max} - 1} \sum_{i=1}^{N_{\text{data}}} W_i(\sigma^{\exp}(E_i) - \sigma(E_i))^2 , \tag{5}$$

was close to unity. In the case when the value of χ^2 was not equal to unity the errors have been renormalized by multiplying by $\sqrt{\chi^2}$. The renormalization does not influence the values of coefficients A_K but manifests itself in changing values of their errors.

The obtained numerical values of coefficients A_k as well as values of coefficients R_i and S_i are available on demand.

4. Parametrization of the angular distributions for elastic scattering

4.1. n+^{1}H and n+^{2}H systems

The logarithm of differential cross section for elastic scattering was represented by a series of the Legendre polynomials $P_L(\cos\vartheta_{\text{cm}})$, thus the differential cross sections can be evaluated according to the formula:

$$\sigma(\vartheta_{\text{cm}}, E) = \exp\left(\sum_{L=0}^{L_{\max}} D_L(E) * P_L(\cos(\vartheta_{\text{cm}}))\right) . \tag{6}$$

The energy dependent expansion coefficients $D_L(E)$ have been determined by the least square fit of the formula (6) to the experimental angular distributions at each given energy "E". The energy dependence of these coefficients was then approximated by the series of the orthogonal polynomials:

$$D_L(E) = \sum_{K=0}^{K_{\max}} C_K^{(L)} Q_K^{(L)}(\tilde{E}) , \tag{7}$$

where $\tilde{E} \equiv E/50 - 1$.

The weights $W_i^{(L)}$ were defined as in formula (3) by reciprocal of the variance of $D_L(E_i)$ coefficients found from the least square fit of the formula (6) to the experimental angular distribution at given energy E_i. Renormalization of weights has been done for the energies E_i at which the best fit of polynomials (6) to experimental angular distribution had produced the χ^2 value significantly different from unity.

The adequate representation of the angular distributions has been obtained with series of Legendre polynomials limited to $L_{\max} = 2$ and 4 for n+^{1}H and n+^{2}H systems, respectively. The quality of the fits is illustrated

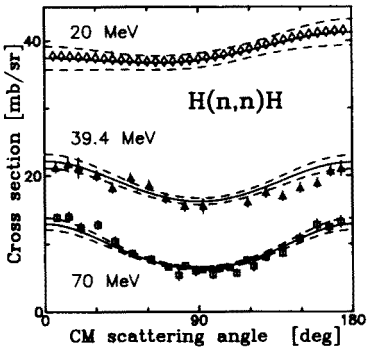

Fig. 2. Comparison of the angular distributions for n+^{1}H elastic scattering, parametrized according to the formula (6), (solid line), with the experimental data (diamonds—Ref. [4], triangles—Ref. [8], squares—Ref. [7]). Dashed lines show the range of three standard deviations of fitted lines.

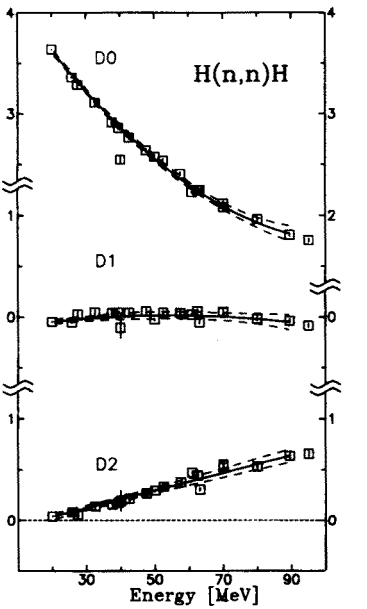

Fig. 3. Energy dependence of expansion coefficients $D_L(E)$, formula (7), for ^{1}H(n, n)^{1}H angular distributions. Dashed lines show the range of three standard deviations of the fitted lines.

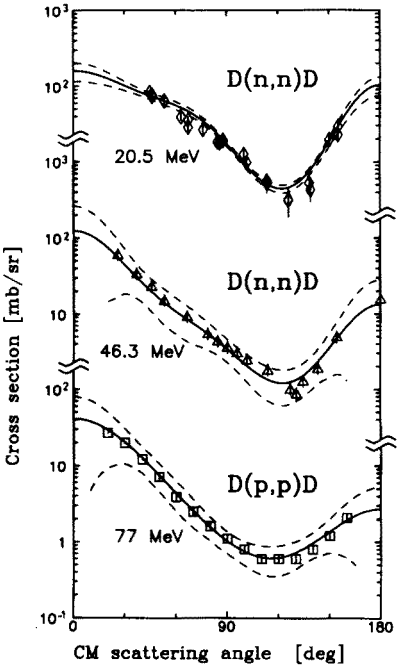

Fig. 4. Comparison of the angular distributions for n+^{2}H elastic scattering, parametrized according to the formula (6) (solid line) with the experimental n+^{2}H data (diamonds—Ref. [14], triangles—Ref. [14]) and with p+^{2}H data (squares—Ref.[21]). Dashed lines show the range of three standard deviations of fitted line.

by Figs 2 and 4 for n+^{1}H and n+^{2}H, respectively, while the energy dependence of the corresponding D_L coefficients is shown in Figs 3 and 5. The obtained numerical values of D_L coefficients are available on demand.

For n+^{1}H scattering the results of this parametrization agree well with those from Ref. [28] in the overlapping energy region up to 30 MeV.

4.2. n+^{12}C system

For the practical use of differential cross sections in the Monte Carlo simulation it is desirable to represent the n+^{12}C data using the same parametrization as for the other nuclei. Therefore, the same procedure was applied for the n+^{12}C scattering as for angular distributions of neutron scattering on ^{1}H and ^{2}H nuclei presented in Section 4.1. The differential cross section was expressed by the formulae (6) and (7). However, instead of experimental cross sections of n+^{12}C scattering the "data" evaluated from the optical model determined as below have been used.

There exist only a few angular distributions for n+^{12}C elastic scattering in energy range 20–40 MeV [29, 30]. Thus the optical model parameters have

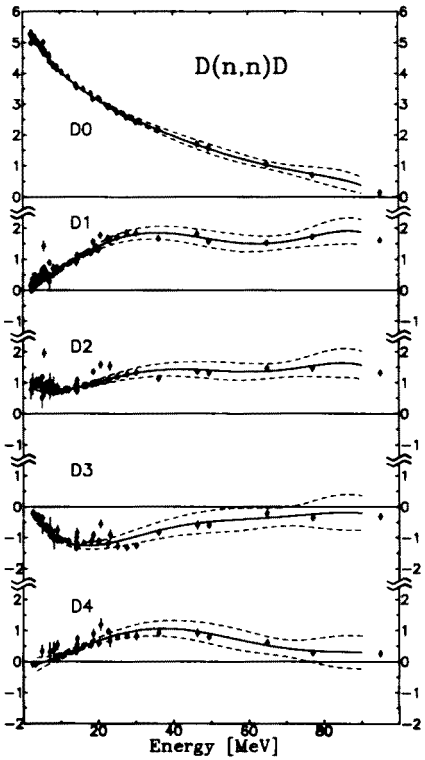

Fig. 5. Energy dependence of expansion coefficients $D_L(E)$, formula (7), for ^{2}H(n, n)^{2}H angular distributions. Dashed line shows the range of 3 standard deviations of fitted line.

been determined from the analysis of proton scattering data on ^{12}C target [5] including both the angular distribution and analyzing power measurements.

The parametrization of the optical model potential was taken with Woods–Saxon formfactors for real and volume imaginary parts, while the derivative of Woods–Saxon form was assumed for the surface part of imaginary potential:

$$V(r) = -U\left[1+\exp\left(\frac{r-R_U}{a_U}\right)\right]^{-1} - iW_{\mathrm{V}}\left[1+\exp\left(\frac{r-R_{W_{\mathrm{V}}}}{a_{W_{\mathrm{V}}}}\right)\right]^{-1}$$

$$-4iW_{\mathrm{S}}\exp\left(\frac{r-R_{W_{\mathrm{S}}}}{a_{W_{\mathrm{S}}}}\right)\left[1+\exp\left(\frac{r-R_{W_{\mathrm{S}}}}{a_{W_{\mathrm{S}}}}\right)\right]^{-2}. \qquad (8)$$

With the energy independent geometrical parameters:

$$R_i = r_i 12^{1/3}; \qquad i = U,\ W_{\mathrm{V}},\ W_{\mathrm{S}},\ \text{so}$$

$$r_U = 1.2336 \text{ fm}, \qquad a_U = 0.6459 \text{ fm},$$

$$r_{W_V} = 0.3497 \text{ fm}, \qquad a_{W_V} = 0.3246 \text{ fm},$$

$$r_{W_S} = 1.2517 \text{ fm}, \qquad a_{W_S} = 0.5537 \text{ fm},$$

the following smooth energy dependence of depth parameters was found in the search:

$$U = (52.095 - 0.4973 \cdot E + 0.00203 \cdot E^2) \text{ MeV},$$

$$W_V = (12.797 + 0.2337 \cdot E - 0.00214 \cdot E^2) \text{ MeV},$$

$$W_S = (4.9454 - 0.0529 \cdot E + 0.00067 \cdot E^2) \text{ MeV},$$

where E is the center of mass energy in MeV.

The Coulomb potential of uniformly charged sphere of radius $R = 1.25 \cdot 12^{1/3}$ fm has been used.

The central potential has been supplemented by the spin-orbit term $V_{so}(r)$ in the Thomas form:

$$V_{so}(r) = -\frac{2V_{so}}{a_{so}} \exp\left(\frac{r - R_{so}}{a_{so}}\right) \left[1 + \exp\left(\frac{r - R_{so}}{a_{so}}\right)\right]^{-2} \tag{9}$$

with energy independent parameters:

$$V_{so} = 6.196 \text{ MeV},$$

$$r_{so} = 0.9792 \text{ fm}, \qquad a_{so} = 0.553 \text{ fm}.$$

The optical model potential presented above gives a good agreement with experimental data from Ref. [5].

This p+^{12}C optical potential with switched-off Coulomb part reproduced well the n+^{12}C differential cross section of elastic scattering as it is shown in Fig. 6 as well as recently published data from Ref. [29]. The somewhat poorer agreement at backward angles (greater than 90°) is probably connected with the presence of some other non-potential scattering mechanism. However, it should be pointed out that the scattering angles greater than 60° give negligible contribution to any Monte Carlo simulation of the scattering process as the probability of the scattering into this angular range is smaller than 2%.

Angular distribution of the n+^{12}C scattering obtained by optical model calculation with the presented above potential in which the Coulomb potential was set equal to zero were parametrized using the same formulae as for n+^{1}H and n+^{2}H angular distributions.

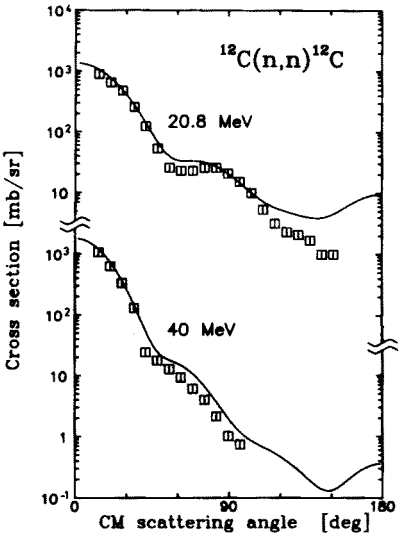

Fig. 6. Comparison of the angular distributions for n+^{12}C elastic scattering, parametrized according to the formula (6) (solid line) with the experimental data from Ref. [29].

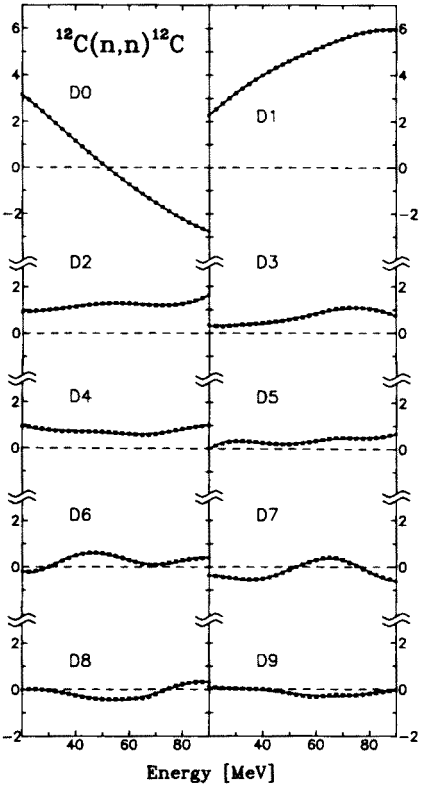

Fig. 7. Energy dependence of expansion coefficients $D_L(E)$, formula (7) for ^{12}C(n, n)^{12}C angular distributions.

The energy dependence of the coefficients D_L of the expansion formula (6) is shown in Fig. 7. The numerical values of the $C_k^{(L)}$ parameters in formula (7) are available on demand.

It should be emphasized that the optical model potential found in this analysis serves only as a tool to obtain parametrization of angular distributions. Thus, no attempt has been made to interpret values of the obtained parameters. However, it is worth to emphasize that very similar values of the parameters have been recently obtained in the analysis of the scattering of polarized protons on light nuclei: ^{13}C, ^{29}Si, ^{31}P Ref. [10] at proton energy 72 MeV.

REFERENCES

[1] F.P. Brady, W.B. Broste, J.C. Wang, J.L. Romero, P. Martens, *Phys. Rev.***C9**, 1784 (1974); J.L. Romero, J.L. Ullmann, F.P. Brady, J.D. Carlson, D.H. Fitzgerald, A.L. Sagle, P.S. Subramanian, C.I. Zanelli, N.S.P. King, M.W. McNaughton, B.E. Bonner, *Phys. Rev.* **C25**, 2214 (1982); H.O. Klages, R. Aures, S.P. Brady, P. Doll, E. Sinckh, J. Hansmeyer, W. Heeringa, J.C. Hiebert, K. Hofmann, H. Krupp, Ch. Maier, W. Nitz, P. Plischke, J. Wilczynski, H. Zankel, B. Zeitnitz, in *Neutron-Nucleus Collisions* AIP Conf. Proc. No 124, 1985 p. 137.; F.P. Brady, P. Doll, G. Sink, W. Heeringa, K. Hofmann, H.O. Klages, W. Nitz, J. Wilczynski, in *6-th International Symposium on Polarization Phenomena in Nuclear Physics,* Osaka 1985, p. 162; H.O. Klages, *Nucl. Phys.* **A463**, 353c (1987).

[2] A. Del Guerra, *Nucl. Instrum.& Methods* **135**, 337 (1976).

[3] Y. Uwamino, K. Shin, M. Fujii, T. Nakamura, *Nucl. Instrum. & Methods* **204**, 179 (1982).

[4] G. Dietze, H. Klein, *Physikalisch-Technische Bundesanstalt,* Braunschweig, Bericht ND-22, 1982.

[5] E. Ieiri, H. Sakaguchi, M. Nakamura, H. Sakamoto, H. Ogawa, M. Yosoi, T. Ichihara, N. Isshiki, Y. Takeuchi, H. Togawa, T. Tsutsumi, S. Hirata, T. Nakano, S. Kobayashi, T. Noro, H. Ikegami, *Nucl. Instrum. & Methods* **A257**, 253 (1987).

[6] A.Ralston, *A First Course in Numerical Analysis,* McGraw-Hill Book Company, Inc. 1965.

[7] J.P. Scanlon, G.H. Stafford, J.J. Thresher, P.H. Bowen, A. Langsford, *Nucl. Phys.* **41**, 401 (1963).

[8] E. Lemon, H. Feshbach, *Rev.Mod.Phys.* **39**, 611 (1967).

[9] J. Hadley, E. Kelly, C. Leith, E. Segre, C. Wiegand, H. York, *Phys. Rev.* **75**, 351 (1949).

[10] B. von Przewoski, P.D. Eversheim, F. Hinterberger, L. Doberitz, J. Campbell, M. Hammans, R. Henneck, W. Lorenzon, M.A. Pickar, I. Sick, *Nucl. Phys.* **A496**, 15 (1989).

[11] N.S.P. King, J.D. Reber, J.L. Romero, D.H. Fitzgerald, J.L. Ullmann, T.S. Subramanian, F.P. Brady, *Phys. Rev.* **C21**, 1185 (1980).
[12] R.A.J. Riddle, A. Langsford, P.H. Bowen, G.C. Cox, *Nucl. Phys.* **61**, 457 (1965).
[13] F.P. Brady, W.J. Knox, R.L. Walraven, J.L. Romero, *Phys. Rev.* **C6**, 1151 (1972).
[14] J.D. Seagrave, J.C. Hopkins, D.R. Dixon, P.W. Keaton Jr., E.C. Kerr, A. Niiler, R.H. Sherman, R.K. Walter, *Ann.Phys.* **74**, 250 (1972).
[15] P. Schwarz, H.O. Klages, P. Doll, B. Haesner, J. Wilczynski, B. Zeitnitz, J. Kecskemeti, *Nucl. Phys.* **A398**, 1 (1983).
[16] A. Horsley, *Nucl. Data Tables* **A4**, 321 (1968).
[17] W.T.H. Van Oers, K.W. Brockman, *Nucl. Phys.* **A92**, 561 (1967).
[18] D.I. Garber, L.G. Stroemberg, M.D. Goldberg, D.E. Cullen, V.M. May, *Angular Distributions in Neutron-Induced Reactions*, Vol. I, Third Edition, BNL-400, January 1970.
[19] H. Shimizu, K. Imai, N. Tamura, K. Nisimura, K. Hatanaka, T. Saito, Y. Koike, Y. Taniguchi, *Nucl. Phys.* **A382**, 242 (1982).
[20] M. Davidson, H.W.K. Hopkins, L. Lyons, D.F. Shaw, *Nucl. Phys.* **45**, 423 (1963).
[21] S.N. Bunker, J.M. Cameron, R.F. Carlson, J. Reginald Richardson, P. Tomas, W.T.H. Van Oers, J.W. Verba, *Nucl. Phys.* **A113**, 461 (1968).
[22] M. Auman, F.P. Brady, J.A. Jungerman, W.J. Knox, M.R. McGie, T.C. Montgomery, *Phys. Rev.* **C5**, 1 (1972).
[23] P.H. Bowen, G.C. Cox, G.B. Huxtable, A. Langsford, J.P. Scanlon, G.H. Stafford, J.J. Thresher, *Nucl. Instrum. & Methods* **17**, 117 (1962).
[24] M.H. MacGregor, W.P. Ball, R. Booth, *Phys. Rev.* **111**, 1155 (1958).
[25] C.I. Zanelli, P.P. Urone, J.L. Romero, F.P. Brady, M.L. Johnson, G.A. Needham, J.L. Ullmann, D.L. Johnson, *Phys. Rev.* **C23**, 1015 (1981).
[26] R.G.P. Voss, R. Wilson, *Proc.R.Soc. London* Ser. A, **236**, 41 (1956).
[27] J. DeJuren, *Phys. Rev.* **77**, 606 (1950).
[28] J.C. Hopkins, G. Breit, *Nucl. Data Tables* **A9**, 137 (1971).
[29] J.S. Petler, M.S. Islam, R.W. Finlay, F.S. Dietrich, *Phys. Rev.* **C32**, 673 (1985).
[30] N. Olsson, B. Trostell, E. Ramström, *Nucl. Phys.* **A496**, 505 (1989).
[31] P.H. Bowen, J.P. Scanlon, G.H. Stafford, J.J. Thresher, P.E. Hodgson, *Nucl. Phys.* **22**, 640 (1961).
[32] T.C. Montgomery, B.E. Bonner, F.P. Brady, W.B. Broste, M.W. McNaughton, *Phys. Rev.* **C16**, 499 (1977).